

Persistence Length of Bounded Actin Bundle

Haosu Tang

April 21, 2013

1 Introduction

The cytoskeleton of the cell is an intricate system of cytoskeletal filaments that supports cell morphology and is crucial for numerous cell functions such as cell motility, cytokinesis and cell division [1, 8, 14]. Three main types of filaments make up the cytoskeleton of eukaryotic cells: intermediate filaments, microtubules and actin filaments. Intermediate filaments provide mechanical strength and resistance to shear stress. Microtubules organize radially within cells and in this way help organize direct intracellular transport and position membrane-enclosed organelles. Actin filaments are more flexible compared to microtubules. They organize into polymerizing and contractile networks and bundles that play a role in determining cell shape during cell motility and division [1].

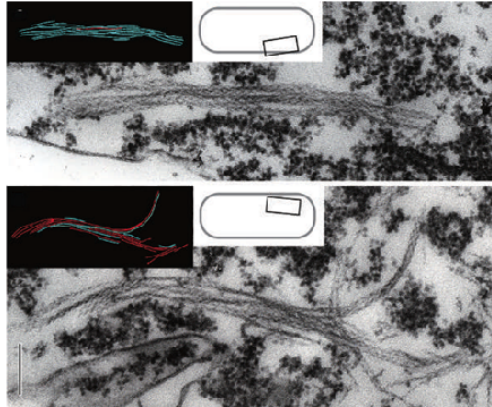


Figure 1: **Actin bundle structure.** Electron microscopy images of S1-decorated F-actin cables in G2 and M phase of *cdc25-22* mutant show that actin cables are bundles of 10 actin filaments (T. Kamasaki et al., *Nature Cell Biol.* (2005)).

The actin filament is a helical fiber made up of actin protein subunits. Interactions between actin filaments and actin associated proteins, such as cross-linking and motor proteins, can lead to complex actin networks that have different structural, dynamical and mechanical properties, such as the actin patches and actin cables (Fig.1). These actin cables are cross-linked by proteins such as α -actinin, fimbrin (plastin) and filamin [13]. The mechanical properties, such as persistence length, bending stiffness of actin bundles are different from that of single actin filaments.

In this work, I study the persistence length of bundled actin filaments from a simulated approach. I used the coarse-grained filament model that I developed in my previous research project (model is described in Sec.3). I redesigned the configurations for this term paper project and all the results from this research are discussed in the following sections.

2 Results

2.1 Bounded actin filament is slightly more flexible

Actin binding proteins that bind to actin filament barbed end can localize at an immobile surface. For example, formin proteins are localized at the fission yeast cell tips and polymerize the actin filament at the barbed end [3,10]. To simulate this process and analyze the mechanical properties of the filament, I fixed the barbed end of the actin filament to a point and investigated the persistence length (PL) under this condition (simulation method described in Section 3.1 and 3.3). PL is calculated by looking at the tangent correlation of the structure. I initialized the actin filament in its equilibrium state. The actin filament then fluctuated and relaxed in the media. The PL was recorded after relaxation shown in Fig.2 in comparison with the unbounded state.

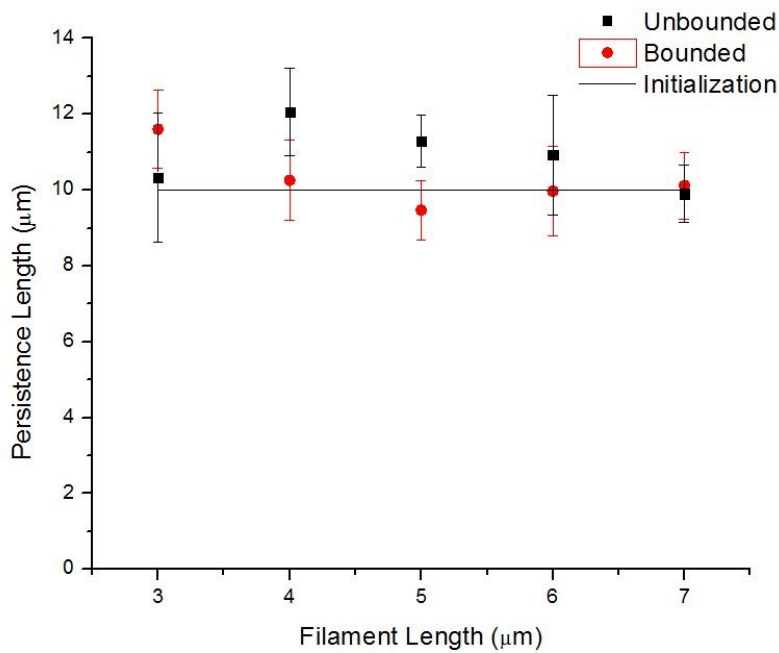


Figure 2: **Persistence length of bounded and unbounded filaments.** Persistence length of unbounded actin filaments (black squares) and bounded actin filaments (red dots) are compared under different filament lengths. Initialization and theoretical equilibrium condition is also shown (black line). The results were calculated after 20s when filaments were relaxed. Error bars are standard deviation from 5 runs.

The PLs of both conditions are close to the preset equilibrium persistence length $10 \mu\text{m}$ (Fig.2). This is because persistence length is a measure of the stiffness only related to the polymer material properties. And material property is not necessarily changed if one end is fixed and the other is free to move. The average PL of unbounded state is $10.90 \mu\text{m}$ while bounded state is slightly (6%) shorter at $10.29 \mu\text{m}$. In simulation, an additional force is added to the first bead to keep the bead fixed, leading to a small structural change. The structural change is passed to the next bead and relax through the whole filament. However, this constant small structural change leads to a slight flexibility increase.

2.2 Bundled actin filaments are stiffer

Actin cross-linking proteins such as α -actinin and fimbrin bundle actin filaments into cables [1]. These actin bundles have much different mechanical properties than individual actin filaments. I calculated the PLs of actin bundles to see how bundling can change these properties. Simulated cross-linking effects are described in Section 3.2.

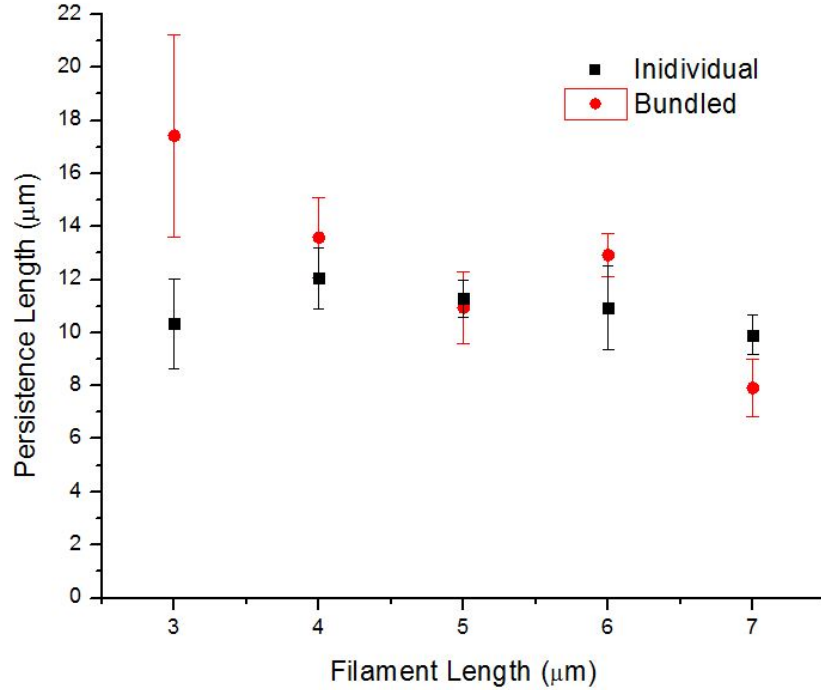


Figure 3: **Persistence length of a actin filament in bundle at 20 s.** Persistence length of individual unbounded actin filaments (black squares) and unbounded actin bundles (red dots) are compared under different filament lengths. The results were calculated at 20 s. Error bars are standard deviation from 5 runs.

5 free actin filaments with different lengths were simulated for 20 s and the PL was calculated and averaged over 5 runs (Fig.3). At $l = 3 \mu\text{m}$, actin bundle is significantly stiffer than individual

actin filament, with PL $17.4 \mu\text{m}$ compared to $10.2 \mu\text{m}$. However, I found that the PLs for bundles with length $4 \mu\text{m}$, $5 \mu\text{m}$, $6 \mu\text{m}$ at 20 s are not too different. For $7 \mu\text{m}$ bundle, the PL is strikingly below the preset value for initialization and equilibrium. This is due to the dynamic “zipping” process I discuss below.

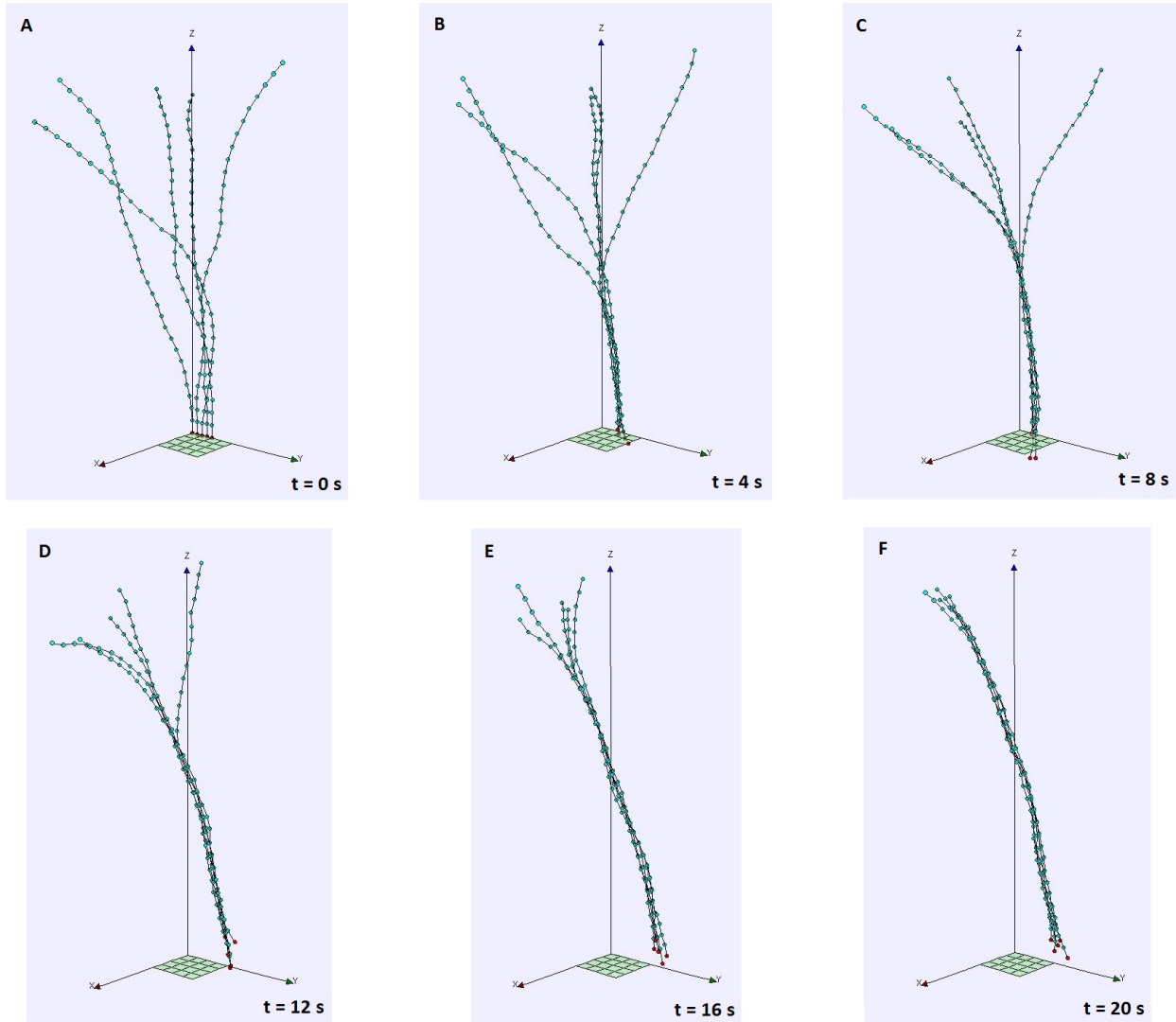


Figure 4: **“Zipping” of actin bundles.** The simulated actin bundle consists of an array of 5 individual actin filaments with length $l = 3 \mu\text{m}$. Screen captures are taken at (A) initialization, (B) $t = 4 \text{ s}$, (C) $t = 8 \text{ s}$, (D) $t = 12 \text{ s}$, (E) $t = 16 \text{ s}$, (F) fully bundled.

Initially, the polymers are simulated randomly under a distribution that would generate a mean fixed persistence length (Fig.4(A)). Therefore, the ends of the filaments are pointed to random directions far away from each other. The first several beads are close to each other, so they interact with each other under cross-linking forces. The cross-linked beads will drag the following beads close to one another and cross-link. Slowly, the cross-linked segment becomes longer like “zip-

ping” (Fig.4(B)-(E)). Finally, the actin filaments are completely cross-linked to a bundle (Fig.4(F)) and fluctuate in this bundled state. A video showing the bounded filaments zipping into bundles: <http://youtu.be/5JOW2FERhWY>.

To test this “zipping” process and its effect on persistence length, I simulated an array of $3\ \mu\text{m}$ filaments and recorded the persistence length change with time (Fig.5).

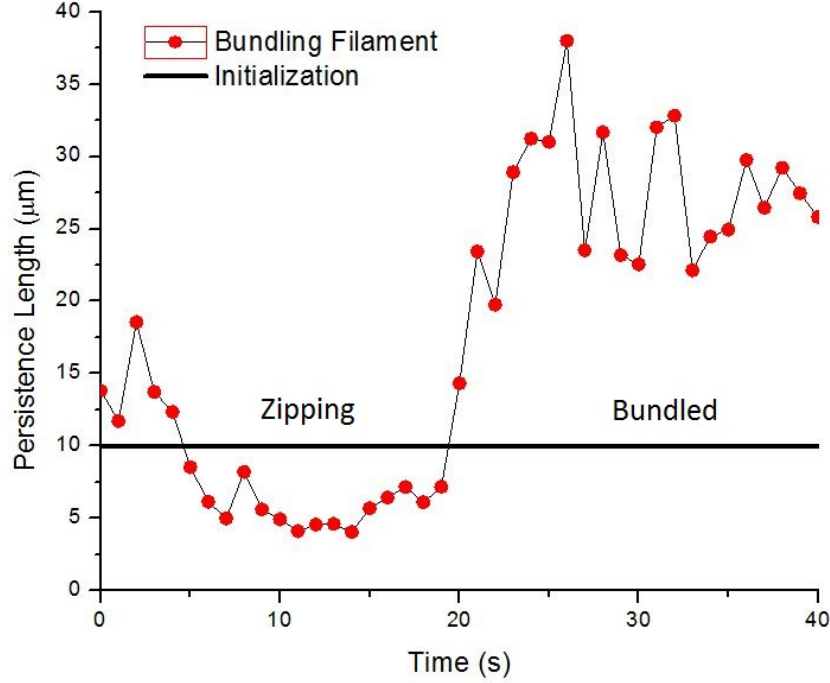


Figure 5: **Persistence lengths of zipping and bundled states.** An array of $5\ l = 3\ \mu\text{m}$ filaments undergo “zipping” and become bundled. According to observation, the filaments become fully bundled at around 20 s. Persistence length of every second is calculated (red dots). Initialization and equilibrium persistence length is set to $10\ \mu\text{m}$ (black line).

The persistence length I calculated is for one of the filament in the bundle. It can only represent the bundle PL when fully bundled (Fig.4(F)). Initially, the filament is independent (Fig.4(A)). During the zipping period (Fig.4(B)-(E)), if the filament end is far away from the bundle, the bundled segment will drag the filament towards the bundle, causing the filament to bend more. This effect is reflected in Fig.5 during the zipping period where the PL is significantly smaller than the PL of the material per se. At the same time, the bending force is trying to overcome the deformation caused by the drag under thermal fluctuation. In the specific case shown in Fig.5 and Fig.4, a stable bundle is formed at around 20 s. The PL by then increases drastically and fluctuates at high level of PL, picturing a very stiff bundle with $\text{PL} \simeq 28.07 \pm 4.30\ \mu\text{m}$.

Therefore, the reason for the observation that long filament bundles at 20 s are more flexible than hypothesized is that these bundles are still under “zipping” process. Once the filaments are

fully bundled, the PLs will be significantly larger than individual filaments.

2.3 Thicker bundles are stiffer

Actin filaments polymerized from the cell tip bundling into cables happens a lot in vivo. For example, Formin proteins that localize at the cell tip polymerize actin filaments in fission yeast [3,10]. These actin filaments then bundle into actin cables under effect of cross-linking proteins [15]. To investigate the mechanical properties of these actin cables, I simulated bounded actin bundles.

The actin bundles are bounded to an array of fixed points on the $z = 0$ plane. Here I looked at filament number ranging from 1 to 6. The first beads are initialized as in Fig.6. The filaments then zip and form bundles. I recorded the PL after observing a complete bundle formation.

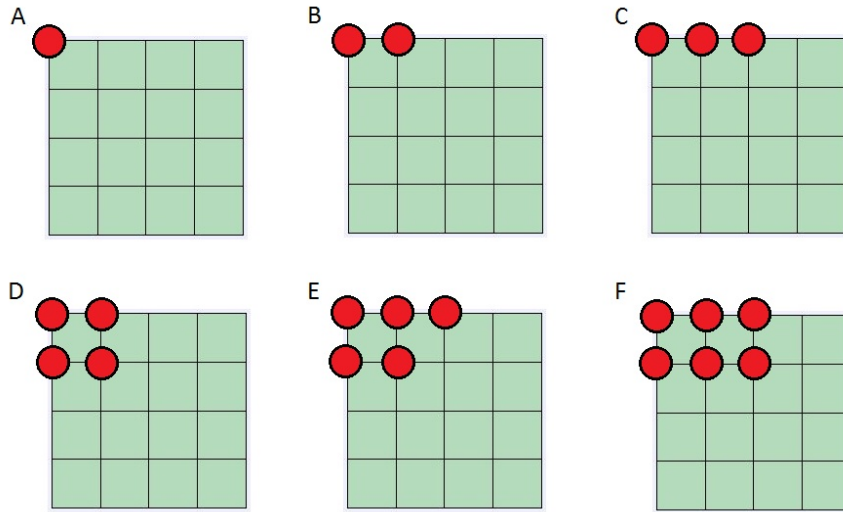


Figure 6: **Schematic of array bundle initialization.** An array of filaments are initialized on the lattice. (A) Individual actin filament. (B)-(F) Bundle of 2 to 6 filaments. The lattice size is $0.05 \mu\text{m}$. Filament length: $3 \mu\text{m}$.

As in Fig.7, the PLs are plotted versus the thickness of the actin bundle. It is obvious that thicker actin bundle would yield stiffer structure, leading to a larger persistence length. An intuitive analogy is for this is if you were to break a twig, thinner ones are easy to break while it takes more strength to break thick branches. The binding energy induced by cross-linking inhibits bending of individual filaments thus making the whole bundle stiffer.

My simulations give insights on how cross-linking into bundles and binding to surface influence the stiffness of the actin filaments. Some quantitative results are shown generated from the simulations and I provided qualitative explanations to them. However, detailed mathematical and physical studies are still lacking. In the work by Claessens *et al.* [2], they showed in experiments that actin-binding proteins can mediate actin filament bundle stiffness. To extend my work, more simulations could be run with longer and thicker actin bundles. Mechanisms such as polymerization can also be added to the simulation to mimic the experimental setups. In fact, a similar ring as in

experiments [2] is formed in my simulation when bundles are confined in a sphere.

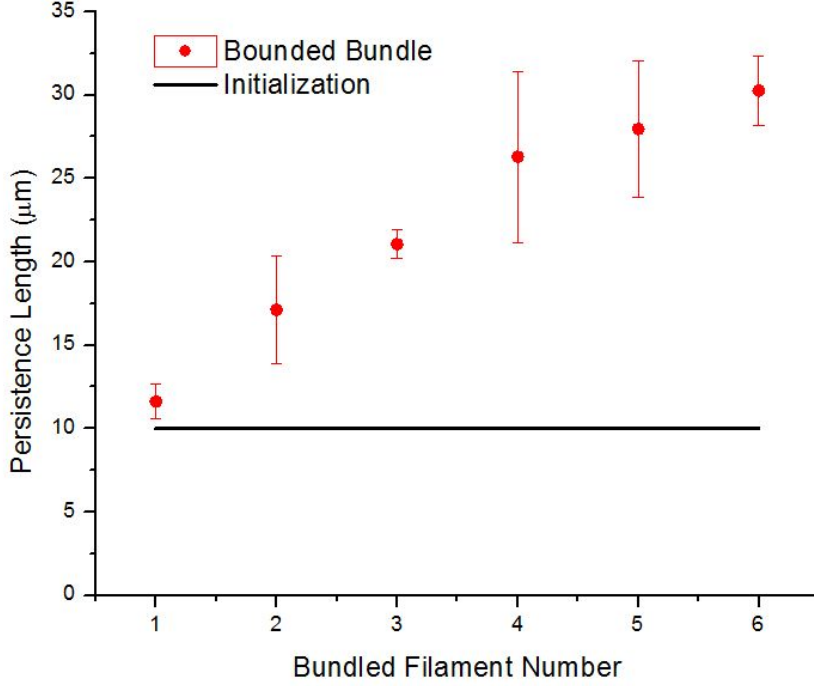


Figure 7: **Persistence length influenced by thickness of bundles.** Persistence length of fully bundled actin filaments (red dots) compared to the initialization and equilibrium preset (black line). Filament length: $3 \mu\text{m}$. Error bars are 5 records of fully bundled filaments fluctuating. A video showing 5 bounded filaments zipping into bundles: <http://youtu.be/5JOW2FERhWY>.

3 Model and Method

3.1 Actin Filament Model

I started by simulating a single filament in 3D space using a bead-spring model [9, 11]. Beads along the backbone of the filament are connected by elastic springs representing the shape of the actin filament (Fig.8(A)).

Spring, bending and thermal forces are the three major forces that control the movement of a free actin filament. Springs have equilibrium length l_0 representing an actin filament segment (typically $0.1 \mu\text{m}$, which is about 37 subunits). The bending force keeps the semi-flexible actin filament in a stable shape. The thermal force simulates fluctuations of the filament. The filament is immersed in a cytoplasmic fluid of viscosity η which I simulate using the Langevin equation of motion [6, 9, 12]:

$$\vec{F}_i^{spring} + \vec{F}_i^{bend} + \vec{F}_i^{thermal} = \zeta_b \frac{d\vec{r}_i}{dt}, \quad i = 1, 2, \dots, N$$

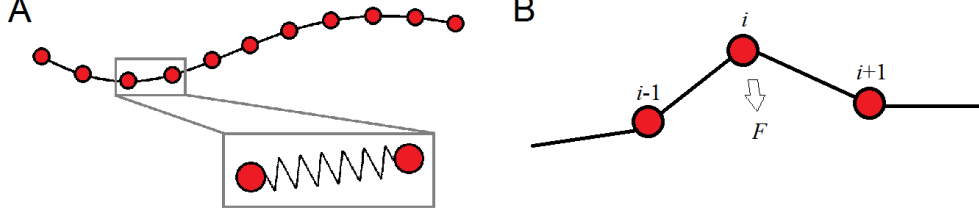


Figure 8: **Model of semi-flexible polymer.** (A) Bead-spring model for actin filament. (B) Bending force.

where \vec{r}_i is the position vector pointing from origin to the i th bead, ζ_b is an effective drag coefficient of a filament segment and the spring, bending and thermal forces are described below.

1. The spring force is calculated from the stretching or compression of the springs between beads [7].

$$\vec{F}_i^{spring} = -\frac{\partial E^{spring}}{\partial \vec{r}_i} = -\frac{k}{2} \sum_{j=1}^{N-1} \frac{\partial (|\vec{r}_{j+1} - \vec{r}_j| - l_0)^2}{\partial \vec{r}_i},$$

where E^{spring} is the total spring energy and l_0 is the equilibrium length. In this case, the i th bead only interacts with two neighboring beads that are connected to it.

2. The bending force is calculated by measuring the deformation of neighboring beads [4, 12](Fig.8).

$$\vec{F}_i^{bend} = -\frac{\partial E^{bend}}{\partial \vec{r}_i} = -\frac{\kappa}{l_0} \sum_{j=2}^{N-1} \frac{\partial (\vec{t}_j \cdot \vec{t}_{j-1})}{\partial \vec{r}_i},$$

where E^{bend} is the elastic bending energy, \vec{t}_i is the local unit tangent vector $\vec{t}_i \equiv \frac{\vec{r}_{i+1} - \vec{r}_i}{|\vec{r}_{i+1} - \vec{r}_i|}$, and κ is the flexural rigidity in thermal equilibrium. One has $\kappa = k_B T l_p$, where k_B is Boltzmann's constant, T is temperature of the environment and l_p is the persistence length of the filament (of order $10 \mu\text{m}$). The bending force on the i th bead is directly related to the positions of the four neighboring beads.

3. The thermal force represents random and thermal forces acting on the filament and satisfy [6]:

$$\langle \vec{F}_i^{thermal} \vec{F}_i^{thermal^T} \rangle_{\alpha, \beta} = \frac{2k_B T \zeta_b}{\Delta t} \hat{I}_{\alpha, \beta},$$

where $\hat{I}_{\alpha, \beta}$ is the second-order unit tensor, and Δt is the simulation time step.

3.2 Cross-linking

Proteins like α -actinin (Ain1p) and fimbrin (Fim1p), bind actin filaments to form actin cables or networks. Here I simulated cross-linking as attraction between beads that come close to one another (Fig.9). The interaction range parameter r_{cross} and interaction strength k_{cross} can be

adjustable in simulations. The cross-linking force, \vec{F}_i^{crslnk} , when bead i is within r_{cross} of bead j (belonging to the same or different filament) is defined as:

$$\vec{F}_i^{crslnk} = -\frac{k_{crslnk}}{2} \sum_j \frac{\partial(|\vec{r}_i - \vec{r}_j| - r_0)^2}{\partial \vec{r}_i}$$

An upper limit to the cross-linking force will be added as in [9].

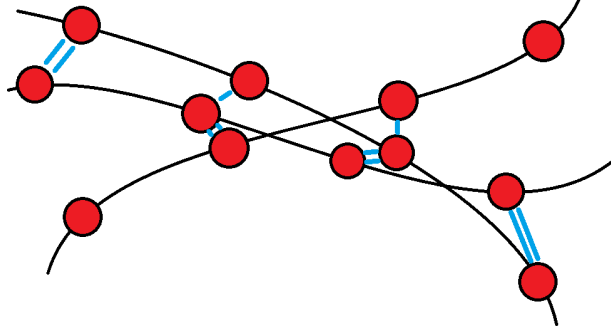


Figure 9: **Cross-linking.** Cross-linking is represented as attraction between neighboring actin filaments.

3.3 Simulation

I developed a java program using Open Source Physics to simulate single actin filament as semi-flexible polymer chain in 3D space. Fig.10(A) shows the initialization of a single actin filament with length $2 \mu m$. The first bead of the filament is at the origin of the coordinates and the second bead is located at $z = l_0$. The surface shown in green indicates $z=0$. An array of actin filaments (Fig.10(B)) are simulated as the first beads align along y-axis with a separation of $0.05 \mu m$.

To simulate a bounded actin filament, I set the first bead fixed at the its original spot while the other beads are free to move or bind.

In the unbounded state, I validated its persistence length in equilibrium. The tangent correlation function $\langle \hat{t}(x) \hat{t}(x + \Delta x) \rangle$ relates to the persistence length of a single filament, which is an important property used as benchmark [5]:

$$\hat{t} = \frac{d\vec{r}}{dx}, \quad \langle \hat{t}(x) \hat{t}(x + \Delta x) \rangle = e^{-\Delta x(D-1)/2l_p}, \quad D \text{ is dimension} = 3.$$

Here x is distance along filament contour. The persistence length is related to the temperature of the environment and to the flexural rigidity κ of the filament, $l_p = k_B T / \kappa$. Experiments show that actin filament has a persistence length of about $10 \mu m$ in vitro [4]. I initialized the filament in its equilibrium state with $l_p = 10 \mu m$. I then tested that the filament has the correct persistence length (Fig.11(A)). After that, I tested that the filament maintains its initial persistence length over times longer than the longest relaxation time and compared to the theoretical result in the above equation (Fig.11(A)).

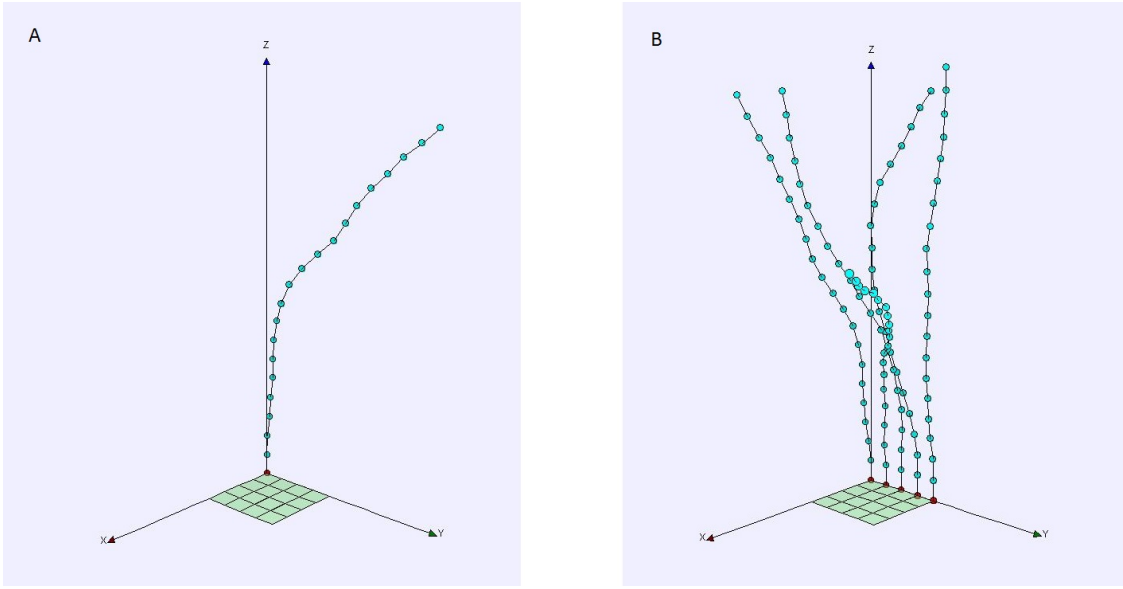


Figure 10: **Simulation initialization.** (A) Initialization of a single actin filament. (B) Initialization of an array of actin filaments. The filaments are $2 \mu\text{m}$ in length. The filaments in the array are separated by $0.1 \mu\text{m}$ for better displaying demonstration, while in real simulations they are separated by $0.05 \mu\text{m}$.

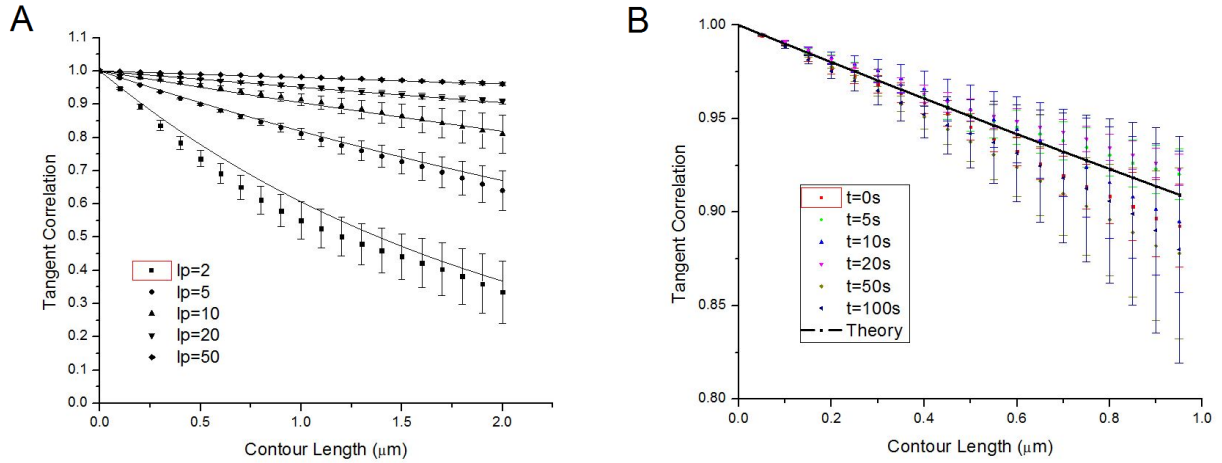


Figure 11: **Tests of simulations using the tangent correlation function.** (A) Tangent correlation function for initialization. Systems are initialized with different persistence lengths l_p in unit of μm . Simulation results (symbols with error bars) are compared with the theoretical results (solid lines). l_p is varied for $2 \mu\text{m}$ (squares), $5 \mu\text{m}$ (dots), $10 \mu\text{m}$ (up triangles), $20 \mu\text{m}$ (down triangles), $50 \mu\text{m}$ (diamonds). Filament length $l = 10 \mu\text{m}$ and $l_0 = 0.1 \mu\text{m}$. Error bars are standard error, 5 runs each. (B) Tangent correlation function as time evolves. $t = 0 \text{ s}$ (red squares), $t = 5 \text{ s}$ (green dots), $t = 10 \text{ s}$ (purple up triangles), $t = 20 \text{ s}$ (magenta down triangles), $t = 50 \text{ s}$ (gold diamonds), $t = 100 \text{ s}$ (blue left triangles) and theoretical values (solid line). Error bars are standard error from 5 runs. Filament length $l = 2 \mu\text{m}$, segment length $l_0 = 0.05 \mu\text{m}$, persistence length $l_p = 10 \mu\text{m}$, with longest relaxation time $t_{relax} \approx 67 \text{ s}$.

References

- [1] Bruce Alberts, Alexander Johnson, Julian Lewis, Martin Raff, Keith Roberts, and Peter Walter. *Molecular biology of the cell*. Garland Science, New York, 4th edition, 2002.
- [2] Mireille M A E. Claessens, Mark Bathe, Erwin Frey, and Andreas R. Bausch. Actin-binding proteins sensitively mediate f-actin bundle stiffness. *Nat Mater*, 5(9):748–753, Sep 2006.
- [3] B. Feierbach and F. Chang. Roles of the fission yeast formin for3p in cell polarity, actin cable formation and symmetric cell division. *Curr. Biol.*, 11:1656–1665, 2001.
- [4] F. Gittes, Mickey B., J. Nettleton, and J. Howard. Flexural rigidity of microtubules and actin filaments measured from thermal fluctuations in shape. *J. Cell Biol.*, 120(4):923–34, 1993.
- [5] Jonathon Howard. *Mechanics of Motor Proteins and the Cytoskeleton*. Sinauer Associates, New York, 2001.
- [6] Taeyoon Kim, Wonmuk Hwang, Hyungsuk Lee, and Roger D Kamm. Computational analysis of viscoelastic properties of crosslinked actin networks. *PLoS Comput Biol*, 5(7):e1000439, Jul 2009.
- [7] H. Kojima, A. Ishijima, and T. Yanagida. Direct measurement of stiffness of single actin filaments with and without tropomyosin by in vitro nanomanipulation. *Proc Natl Acad Sci U S A*, 91(26):12962–12966, Dec 1994.
- [8] David R Kovar, Vladimir Sirotkin, and Matthew Lord. Three’s company: the fission yeast actin cytoskeleton. *Trends Cell Biol*, 21(3):177–187, Mar 2011.
- [9] Damien Laporte, Nikola Ojkic, Dimitrios Vavylonis, and Jian-Qiu Wu. -actinin and fimbrin cooperate with myosin ii to organize actomyosin bundles during contractile-ring assembly. *Mol Biol Cell*, 23(16):3094–3110, Aug 2012.
- [10] S. G. Martin and F. Chang. Dynamics of the formin for3p in actin cable assembly. *Curr. Biol.*, 16:1161–1170, 2006.
- [11] F. J. Ndlec, T. Surrey, A. C. Maggs, and S. Leibler. Self-organization of microtubules and motors. *Nature*, 389:305–308, 1997.
- [12] M. Pasquali, V. Shankar, and D. C. Morse. Viscoelasticity of dilute solutions of semiflexible polymers. *Phys. Rev. E*, 64:020802, 2001.
- [13] T. D. Pollard and J. A. Cooper. Actin and actin-binding proteins. a critical evaluation of mechanisms and functions. *Annu. Rev. Biochem.*, 55:987–1035, 1986.
- [14] Thomas D. Pollard and William C. Earnshaw. *Cell biology*. Saunders, Philadelphia, 2004.
- [15] Colleen T Skau, David S Courson, Andrew J Bestul, Jonathan D Winkelman, Ronald S Rock, Vladimir Sirotkin, and David R Kovar. Actin filament bundling by fimbrin is important for endocytosis, cytokinesis, and polarization in fission yeast. *Journal of Biological Chemistry*, 286(30):26964–26977, 2011.